

# A pseudo-genetic stochastic model to generate karstic networks

Andrea Borghi<sup>a,\*</sup>, Philippe Renard<sup>a</sup>, Sandra Jenni<sup>b,1</sup>

<sup>a</sup>University of Neuchâtel, Stochastic Hydrogeology Group, 11 Rue Emile Argand, CP 158, 2000 Neuchâtel, Switzerland

<sup>b</sup>Schlumberger Water Services, Immeuble Madeleine D, 92057 Paris la Défense Cédex, France

## S U M M A R Y

In this paper, we present a methodology for the stochastic simulation of 3D karstic conduits accounting for conceptual knowledge about the speleogenesis processes and accounting for a wide variety of field measurements.

The methodology consists of four main steps. First, a 3D geological model of the region is built. The second step consists in the stochastic modeling of the internal heterogeneity of the karst formations (e.g. initial fracturation, bedding planes, inception horizons, etc.). Then a study of the regional hydrology/hydrogeology is conducted to identify the potential inlets and outlets of the system, the base levels and the possibility of having different phases of karstification. The last step consists in generating the conduits in an iterative manner using a fast marching algorithm. In most of these steps, a probabilistic model can be used to represent the degree of knowledge available and the remaining uncertainty depending on the data at hand.

The conduits are assumed to follow minimum effort paths in a heterogeneous medium from sinkholes or dolines toward springs. The search of the shortest path is performed using a fast marching algorithm. This process can be iterative, allowing to account for the presence of already simulated conduits and to produce a hierarchical network.

The final result is a stochastic ensemble of 3D karst reservoir models that are all constrained by the regional geology the local heterogeneities and the regional flow conditions. These networks can then be used to simulate flow and transport. Several levels of uncertainty can be considered (large scale geological structures, local heterogeneity, position of possible inlets and outlets, phases of karstification).

Compared to other techniques, this method is fast, to account for the main factors controlling the 3D geometry of the network, and to allow conditioning from available field observations.

*Keywords:* Karst, Conduit network, Stochastic simulation, Geological modeling, Reservoir modeling, Fractures modeling

## 1. Introduction

Karst formations are estimated to cover about 20% of the land surface of the world (Ford and Williams, 2007) and 35% of Europe (Biondic and Bakalowicz, 1995). According to these last authors, they constitute the main water resource in Europe and have therefore a crucial importance. However, they are difficult to characterize because of their extreme heterogeneity induced by the presence of sparse conduits embedded in a fractured carbonate matrix. Worthington et al. (2000) reviews of four typical karst aquifers in which more than 90% of the flow occurs in the conduits while more than 90% of the water is stored in the fractured matrix. It is therefore crucial to account both for the matrix and the con-

duits when modeling these aquifers for groundwater protection, management, or to investigate contamination issues. Including the conduits in the formulation of the numerical models has been pioneered by Kiraly (1979, 1988) and is still a topic of active research (Cornaton and Perrochet, 2002; Eisenlohr et al., 1997; Hill et al., 2010; Jourde et al., 2002; Sauter et al., 2006). These authors provide various numerical techniques to account for the conduits and discuss the different types of flow and transport equations that can be used in the conduits and in the matrix.

In this paper, we take a different perspective. Indeed, a major difficulty when modeling karst aquifers is that the location of the conduits is often unknown since they are seldom hit by boreholes and are difficult to detect by geophysical techniques when their diameter is small. We therefore propose a method to model the possible occurrence of the conduits. Once the conduits are modeled, they can be used as input for flow and transport models. Modeling the possible occurrence of the conduits can also be used directly to assess the risk of conduit occurrence in mining or geo-technical projects involving for example tunnels or dams (e.g. Filipponi and Jeannin, 2010). All these potential applications will not be discussed in detail or tested by the present paper.

\* Corresponding author. Address: CHYN-Hydrogeology Center, University of Neuchâtel, Stochastic Hydrogeology Group, 11 Rue Emile Argand, CP 158, 2000 Neuchâtel, Switzerland. Tel.: +41 79 475 18 89.

E-mail addresses: andrea.borghi@unine.ch (A. Borghi), philippe.renard@unine.ch (P. Renard).

<sup>1</sup> Present address: Agence Nationale pour la Gestion des Déchets Radioactifs, 1/7 Rue Jean Monnet, 92290 Châtenay Malabry, France.

So far, only a few techniques have been developed to model the structure of karst conduit networks. The most advanced ones are based on modeling the physics and chemistry of the speleogenesis processes (Dreybrodt et al., 2005; Kaufmann and Braun, 2000). This approach allows understanding the kinetics of karst evolution, and give precious information about the speleogenesis processes. However it is difficult to apply to model in order to characterize an actual system, mainly because it is difficult to reconstruct the paleoclimatic and geological conditions that were prevailing during its formation. Consequently, these models are extremely difficult to condition to field observations. In addition, they are very CPU demanding, because they are based on the numerical solution of highly nonlinear and coupled systems of equations. For this reason, these models are usually not applied in a Monte-Carlo framework allowing site characterization and risk analysis. Another approach is to build a purely statistical model. For example, Henrion et al. (2008) and Henrion et al. (2010) propose to model complex cave geometries by generating first a stochastic discrete fracture network and then combining it with a truncated multi-Gaussian field in order to represent the 3D geometry of the caves around the conduit network. An intermediate type of model is proposed by Jaquet et al. (2004). They use a modified lattice-gas automaton for the discrete simulation of karstic networks. By this approach, walkers are sent through the medium and erode it progressively. The hierarchical structure is modeled by attracting the walkers by the conduit system simulated at the previous iteration. This technique is also very difficult to condition to field data because of the random walk technique. Ronayne and Gorelick (2006) propose to simulate branching channels (analogous to karst conduits) using a nonlooping invasion percolation model. This method is used to investigate the effective property of media presenting such type of structures but it is not designed to model a specific site and to be conditioned by field observations (known presence of conduits in boreholes, dolines, sinkholes, etc.).

In this paper, we propose a new methodology that aims at simulating the geometry of karstic conduits at a regional scale constrained by the regional geology, by the regional hydrological and hydrogeological knowledge, and by a conceptual knowledge of the genetic factors (like e.g. fracturation, bedding planes) that control the conduit genesis, without solving the physical and chemical equations of the speleogenesis. The motivation is to include those processes in a simplified manner to ensure that the modeled geometry is realistic while being sufficiently numerically efficient to allow a stochastic analysis. The proposed methodology is based on the assumption that water and karst conduits will follow a minimum effort path which is computed using a fast-marching algorithm (Sethian, 1996). The generation of the conduits is performed in a stochastic framework allowing to generate multiple equiprobable realizations that are all conditioned by field observations (dolines, sinkholes, presence of caves in boreholes, known interconnected springs and sinkholes, etc.).

After describing the principle of the methodology in Section 2 and its implementation in Section 3, the paper presents two illustrations of the method. One in a coastal aquifer along the Mediterranean coast and one for the Noiraigue spring catchment in the Swiss Jura Mountains, close to the city of Neuchâtel. This last example has been chosen because an important data set is available from previous studies (Atteia et al., 1998; Gogniat, 1995; Morel, 1976) and because its structural geology is complex (Valley et al., 2004).

## 2. Overview of the approach

Before describing the details of our approach, we provide an overview of the underlying conceptual model and of the rationale behind the proposed methodology.

Different conceptual models have been developed in the last century to describe the factors that control the formation of karst structures; they are reviewed by Ford and Williams (2007). According to Klimchouk (2007), one can distinguish two main types of karsts. Hypogenetic karst aquifers are formed under deep conditions mainly by hydrothermal waters while epigenetic karst aquifers are formed under surface conditions by the circulation of rainfall water.

The methodology discussed in the present paper focuses on epigenetic karsts. They can be divided in three distinct zones. The first is the unsaturated (vadose) zone. It can be very deep for mature karst aquifers (according to Ford and Williams, 2007, several hundreds of meters). In this zone, karst conduits are mainly subvertical because gravity is the most influent factor. Then these subvertical conduits reach the phreatic (by definition saturated) zone. They become more and more concentrated leading to a hierarchical structured network (Jeannin, 1996) which leads toward one or more springs. The epiphreatic (intermittently saturated) zone is located between the vadose and phreatic zones. It is the zone which is saturated under high flow conditions. It can be formed by old phreatic conduits or by subvertical vadose conduits (Ford and Williams, 2007). Because of their organized structure, the connectivity of the karst conduit network is very strong, and therefore crucial to understand the flow and transport phenomena. Furthermore karst aquifers have a superficial zone, called epikarst (a few meters below topographic surface). This superficial zone collects rainfall water and redirect it toward the vadose conduits. Typically, dolines are points where epikarstic water is concentrated in a preferential inlet.

The epikarstic layer will not be taken into account in this methodology, because it focuses on the geometrical modeling of the main karst conduits. In epigenetic karst aquifers, the density and geometry of the karst conduits depend on two main factors. The first is the geology that controls their shape and distribution: conduits are formed by dissolution. This process is predominant in limestones and other highly soluble rocks like evaporites and are preferentially located along bedding planes and/or initial fracturation (Filipponi et al., 2009; Palmer, 1991; Worthington, 1999). The second factor is the hydrology that controls recharge and the position of recent or paleo base levels (Bakalowicz, 2005). These two factors interact during the formation of the karst network leading a final distribution of conduit orientations in 3D that is different from the orientations of the fractures alone (Kiraly et al., 1971). The simulation of the speleogenesis processes has shown in addition (Dreybrodt et al., 2005) that the increased conductivity of the conduits, that are formed progressively during the evolution of the system, re-orient the flow field and the preferential areas of dissolution leading then to a hierarchical structure.

Overall, to account for all the constraints described above in a simplified manner, the proposed methodology consists of four main steps (Fig. 1): modeling the regional geology, modeling the fracturation and bedding planes within the regional geology, analyzing the hydrological control, and finally modeling the conduits. The concepts underlying these four steps and the choices that have been made are presented in the following subsections while their implementation is described in Section 3.

### 2.1. Regional geology modeling

The first major control on the formation of karstic network is the regional geology (i.e. the location of the aquitards and carbonate formations). The first step consists therefore in modeling the regional scale structures, i.e. modeling the sedimentary and tectonic structure. The extension of the model has to be decided carefully. It must take into account both the topographical and hydrogeological catchment. Furthermore, it is better to extend

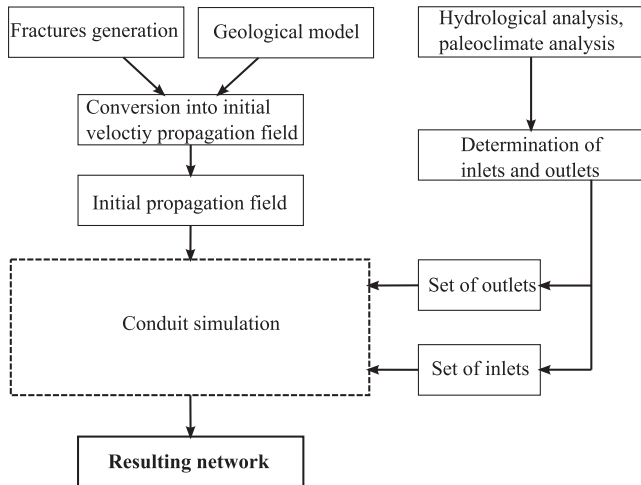


**Fig. 1.** Workflow of the complete algorithm, the input are the fracture model, the geological model and the hydrogeological analysis. After a preprocessing step they pass through the conduit simulation box (see Fig. 5) and finally the resulting network is obtained.

the model to take into account for possible complex 3D flow paths. As a side remark, the geological model can be used to estimate more accurately the catchment extension in surface (Borghi, 2008). For example, if an aquitard formation underlies a karstic formation, the axis of the anticline on the top of the aquitard can be used to draw a reasonable estimation of the boundary of the catchment.

During that step, an accurate study of the stratigraphic or sedimentary units is fundamental because the conduits will develop only in carbonates and other highly soluble formations. Once this information is acquired, it allows defining how the stratigraphic units will be grouped. The aim is to construct a geological model of the hydrogeological formations based on their hydrogeological properties rather than their age.

Once the hydro-stratigraphy is defined, the geological structure has to be modeled because the karstic network will be strongly constrained by the structure (folds, faults and thrusts). A good structural interpretation is therefore a key prerequisite to build a realistic 3D geological model.

From a technical point of view, different 3D geological modeling techniques and software are available (Calcagno et al., 2008; Caumon et al., 2009; Lajaunie et al., 1997; Mallet, 2002). The important point is that one should select a technique which ensures that the modeled volumes are coherent. Models that are only based on the 3D modeling of the surfaces bounding the formation may not ensure this coherence if they do not account for topological constraints. They may for example not ensure the exact definition of closed volumes and will not be applicable in the following steps of the methodology. This is particularly important in highly deformed areas such as the “Vallée des Ponts-de-Martel” (Section 4.2) where thrusts, folds and faults can create hydraulic contact or barrier between two different aquifers that would normally be separated by an aquitard. In summary, one should select a 3D modeling technique allowing to account for the degree of complexity of the geological structure present in the studied site while ensuring the 3D volume coherence.

## 2.2. Fracturation and bedding planes

As described in Filipponi (2009), the karst conduits shape and density are strongly influenced by the properties of the geological formations in which they develop. These characteristics, fractur-

ation and bedding planes, can be inferred from borehole data (for deep reservoirs) or outcrop analysis when they are expected to be representative of the fractures at depth (Sharp et al., 2006).

### 2.2.1. Fracturation

The fracturation of the rock influences the orientation of the conduits and their path (Palmer, 1991). From a geometrical point of view, a fracture network is usually decomposed in a number of fracture families. Each family is then described statistically by a density or spacing, ranges of orientation, length or size distribution, relationship between the fracture density and stratigraphy. The types of geometrical relations between the fracture families can also be important (Kaufmann, 2009). All those properties control the connectivity of the system and have a strong influence on the initialization of the karst conduits (Ghosh and Mitra, 2009). In addition, according to (Gillespie et al., 1993) two additional characteristics influence the flow properties of the medium: fracture roughness and fracture aperture.

Once the field data have been acquired, a classical approach is to use stochastic discrete fracture network models. Different methods have been developed, from the most simple Boolean model of uniformly distributed fractures of identical size (monodisperse case) to complex models allowing the inclusion of several fracture families, variable density in space and various types of relations between the families (Bour et al., 2002; Castaing et al., 2002; Gringarten, 1998). Among the most advanced techniques, some authors propose to estimate the local density and orientation of the fractures by using numerical codes allowing to compute rock deformation and geomechanical stresses (Camac and Hunt, 2009).

### 2.2.2. Inception horizons

Filipponi (2009) shows that particular horizons within a sedimentary formation have a very strong importance during the activation process of the cave genesis. These horizons, called inception horizons, present either a particular capability to be dissolved or a specific contrast with the surrounding rock (chemical, mineralogical or rheological). The inception horizons are therefore specific stratification joints or bedding plane. As a result, like for the fracturation, the location of the inception horizons or stratification joints within a karstifiable formation is a key heterogeneity factor that controls the geometry and position of the conduits. They must therefore be accounted for in the model either in a statistical or deterministic manner. In our approach, the location of the inception horizons is inferred from the geological model. They are considered to be parallel to the main sedimentary structure. In the field, the location of these horizons can be identified and measured along outcrops.

## 2.3. Hydrodynamic control

While the two factors described above are related to the static structure of the medium, the third main factor controlling the geometry of a Karstic network is related to the hydrological and (paleo) climatic situation at the site (see classification by Palmer, 1991). The amount of recharge controls the degree of karstification (Bakalowicz, 2005) and its spatial distribution controls the type of karstic network that can be expected. The presence of a base level controls the position of the outlets and the limit between the vadose and phreatic zones. In presence of seawater, the position of the interface with freshwater will be a zone of preferential dissolution due to chemical in equilibrium resulting from the mixing of fresh and salt waters (Dreybrodt Malaga, 2010, p. 457). All these constraints can change in time and space leading to different stages of karstification. Consequently a good knowledge of the paleo and actual conditions is required to understand and simulate the different stages of karstification.

The information concerning the hydrodynamic control can be obtained from classical hydrogeological analysis, tracers tests, recharge and geomorphological studies. At the end of this analysis one should know: the extension of the catchment, the location of the actual and possible paleo outlet(s), the type of recharge (diffuse–punctual), the map of the zones of recharge (known point, possible points, and diffuse areas) and the overall water balance of the catchment basin.

### 2.3.1. Hydrogeological analysis

In that part of the work, the aim is to collect all the information available related to the position of the known inlets and outlets in order to define where they are located and how they should be modeled (punctual or diffuse).

The paleo (several hundreds of thousands of years, i.e. glacial periods) recharge and base level conditions should be estimated as well, at least approximatively, in addition to the actual ones. This allows to identify the possible existence of different stages of karstification and to model them. For example, the “Sieben Hengste” karstic network was formed at least under three different hydrological conditions (Jeannin, 1996). The change of the regional hydrologic base level has then triggered the generation and reactivation of different families of conduits resulting in a complex structure that cannot be understood without knowing these different stages (Filipponi, 2009).

### 2.3.2. Recharge analysis

In the proposed procedure, the water balance of the catchment must be analyzed for two reasons. First, the water balance of the catchment allows to check whether the size of the catchment is in agreement with the total discharge at the outlets. On the other hand, the water balance can also be used to check whether all the outlets of a given catchment have been identified. If there is more inflow than outflow, one can be sure that there are other outlets which may be hidden or diffuse and more hydrogeological research should be done to clarify the situation before starting to make a model. There is a second reason to analyze recharge: it is that the type of networks that are expected at a given location will be different depending on the type of recharge. Palmer (1991) considers mainly three different types of recharge: via karst depressions, diffuse (through porous rocks) and hypogenic (acids). In the first case one may expect a branchwork type of network, in the second case it should be an anastomotic or network maze, while on the third case one would expect more a spongework maze or ramiform pattern. Identifying the different types of recharge can be based on field observations and supported by water balance calculation. Numerical modeling can help in this process. For example, Borghi (2008) used a finite element method to solve the steady state flow based on mean annual recharge values using an equivalent hydraulic conductivity for the different hydrogeological units (based on a 3D geological model). This allowed identifying the different recharge/discharge zones of the Noiraigue's catchment. He showed in that case that a significant proportion of the recharge (30%) was diffuse through the sandstone aquitard located over the karstic aquifer.

### 2.3.3. Geomorphological analysis

While the most important inlet and outlet are often known from field observations and their relation confirmed by tracer tests, many smaller inlets are not known precisely. Still some must be modeled and their location should be estimated. This is why we propose to complement the classical hydrogeological analysis with a geomorphological study. The underlying concept is that punctual inlets (dolines and sinkholes) create geomorphological depressions; an accurate geomorphological analysis of the landscape allows identifying them. This can be partly automated using high

resolution digital elevation model and numerical algorithms (Lamelas et al., 2007), but it needs to be controlled in the field if possible.

### 2.3.4. Tracer tests

Tracer tests are often used in karst studies (Käss, 1998; Leibundgut et al., 2009). Here we use their results in a two manners. First, they are used to delineate the extension of the catchment by showing which inlets are connected to the outlets of interest. Second, this connectivity information is used during the simulation process to ensure that points known to be connected from field observations will also be connected in the model. The model should however be flexible enough to account for the fact that the same sinkhole can be connected to many springs and vice versa (i.e. spring connected to many sinkholes).

## 2.4. Karst conduit simulation

The final step of the proposed methodology is the simulation of the karstic network. The method is inspired by speleogenetic process based models (Dreybrodt et al., 2005; Kaufmann and Braun, 2000). In order to accelerate the simulation, we use a proxy allowing to mimic the final result (mature system) without modeling the physical and chemical processes.

The proxy is based on the assumption that water, and thus karst conduits, will follow the minimum effort path, i.e. the path that is the most convenient for flow between inlets and outlets. In a homogeneous medium, it would be a straight line between sinkholes and the spring. In reality, however, it depends on the pre-existing geological heterogeneity and follows more complex paths.

The computation of these paths is based on a Fast-Marching Algorithm (FMA) (Sethian, 1996, 1999, 2001). We assume the karst spring to be the starting location of the FMA. The result is a map of the minimum time required to reach the spring. We then we perform a particle tracking starting from the sinkholes (or dolines) toward the spring. The particle follows the shortest path and “corrode” the model in a manner similar to Jaquet (2004). The resulting path becomes one of the karst conduits. Section 3.4 explains the implementation in detail.

## 3. The proposed algorithm and its implementation

This section describes in detail the four main steps of the methodology: geological modeling, heterogeneity modeling, hydrogeological analysis and simulation of karst networks. We use two 2D synthetic cases (one vertical cross-section and one horizontal map) for illustration.

The simulation framework is composed of a deterministic and a stochastic component. To differentiate them, we use the superscript “S” to denote the variables that are realizations of a stochastic process.

### 3.1. 3D geological model

The first step of the methodology is to build a 3D geological model of the catchment area. Mathematically, and in a very general manner, we consider that the 3D model is represented by a set of indicator functions allowing to know which is the geology present in any position  $\vec{x} = (x, y, z)$

$$I_C(\vec{x}, \vec{g}) = \begin{cases} 1, & \text{if geology } g \text{ is present at location } \vec{x} \\ 0, & \text{otherwise} \end{cases} \quad (1)$$

where  $g = \{1, \dots, N_g\}$  is the geological facies, with  $N_g$  the number of lithological facies.

This function can be obtained from a wide variety of interpolation methods and modeling tools. In the example and the case study that are discussed in Section 4, we used the software Geomodeler3D (Calcagno et al., 2008). It is based on an implicit method (Lajaunie et al., 1997) particularly well suited for the complex geology of the Jura because it allows accounting for the structural data (strikes and dips) not necessarily measured along a geological interface.

### 3.2. Internal structure of the carbonates

Here, the aim is to obtain an indicator function of the internal heterogeneities of the carbonates due to fracturation and bedding planes. As for the geology, we define a set of indicator functions.

$$I_F^S(\vec{x}, f) = \begin{cases} 1, & \text{if fracture } f \text{ is present at location } \vec{x} \\ 0, & \text{otherwise} \end{cases} \quad (2)$$

where  $f = \{1, \dots, N_f\}$  is the fracture or bedding plane family,  $N_f$  the number of codes defining which class of heterogeneity is present and the superscript  $S$  means that it is an equiprobable realization of a stochastic model (Fig. 2).

There are many ways to generate the fracture network. In the following examples, we use a simple Boolean object model for the fractures and rasterize it on a regular rectangular grid. The fracture model could be much more complex, but this would not change the overall methodology. More precisely, we assume that there is a finite number of fracture families  $N_f$ . For each fracture family, the parameters of our model are a probability of occurrence (density), and a range of dip, strike, and fracture length. In practice, the coordinates of the centroid of every fracture is randomly sampled in a uniform distribution within the 3D model. The fracture length is uniformly sampled between a minimum and a maximum values as well as the dip and the strike. The number of families and their statistical parameters are provided by the user.

Furthermore, we consider bedding planes according to Filipponi (2009) as inception horizons. These horizons are considered in the same way as fractures, i.e. as cells with increased permeability. They can also be modeled stochastically. In this case, they are assumed to be the surfaces of iso-thickness dividing the karstic formation. Their value of iso-thickness is sampled randomly as a relative thickness of the karstic formation.

### 3.3. Hydrogeological analysis

Determining the inlets and outlets of a karst aquifer is a key step in the procedure because the karst conduits will be constructed (Section 3.4) as the paths connecting the inlets and outlets.

#### 3.3.1. Inlets of the system

A hydrogeological analysis of the system must be carried out to identify the inlets of the system (dolines, sinkholes, etc.). These points are located on the topography. Among them some are known from the hydrogeological studies: main sinkhole for example or points identified by tracer tests. Their location is deterministic. However, we consider that there is also a number of potential inlets on the topography whose location has not been confirmed by field observations. For those points, we use a stochastic point process model.

The set of  $N_D$  deterministic inlets is denoted by  $\mathfrak{I}_D$ .

$$\mathfrak{I}_D = \{(x_i, y_i, z_i) \text{ with } i \in (1, \dots, N_D)\} \quad (3)$$

For each realization, the set of  $N_p$  potential inlet locations  $\mathfrak{I}_p^S$  is generated randomly based on a map of probability of occurrence  $Pi_3(x, y)$  derived from field observations and from analysis of the recharge process (Section 2.3).

$$\mathfrak{I}_p^S = \{(x_i, y_i, z_i) \text{ with } i \in (1, \dots, N_p)\} \quad (4)$$

Finally the complete set of inlets  $\mathfrak{I}^S$  for each realization  $S$  is the union of  $\mathfrak{I}_D$  and  $\mathfrak{I}_p^S$

$$\mathfrak{I}^S = \mathfrak{I}_D \cup \mathfrak{I}_p^S \quad (5)$$

Furthermore, we mark each inlet point with an importance factor  $w_i^3$ . It is proportional to the upstream drained area  $C_i$  computed using the Digital Elevation Model of the area and the matlab Topo-Toolbox (Schwanghart and Kuhn, 2010). We then define the importance factor for every single inlet  $w_i^3$  as the percentage of the total catchment area  $C_{tot}$  that it drains.

$$w_i^3 = \frac{C_i}{C_{tot}} \quad \forall i \in (1, \dots, N_3) \quad | \quad N_3 = N_p + N_D \quad (6)$$

#### 3.3.2. Outlets of the system

The second aim of the hydrogeological analysis is to identify the major outlets of the system (springs and spring zones). As well as the inlets, the deterministic outlets will be identified as a set  $O_D$  of  $N_{OD}$  points defined as follows:

$$O_D = \{(x_i, y_i, z_i) \text{ with } i \in (1, \dots, N_{OD})\} \quad (7)$$

And the set of  $N_{OP}$  potential outlets  $O_p^S$  is generated randomly based on a probability map of occurrence  $Pi_O(x, y)$  derived from field observations and from topographical analysis of the catchment.

$$O_p^S = \{(x_i, y_i, z_i) \text{ with } i \in (1, \dots, N_{OP})\} \quad (8)$$

finally the complete set of outlets  $O^S$  for each realization  $S$  is the union of  $O_D$  and  $O_p^S$

$$O^S = O_D \cup O_p^S \quad (9)$$

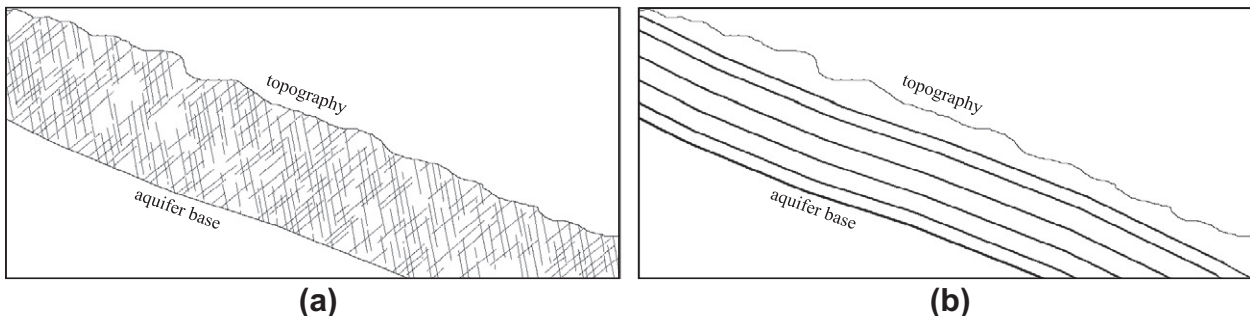


Fig. 2. 2D cross-section: (a) simple fracture model with two families of fractures, the fracture model is applied only in the karstifiable formation, (b) bedding planes in the karstifiable formation.

### 3.4. Karstic network modeling

In every simulation, the karstic network is generated using walkers that follow a shortest path to the spring. The path accounts for the local heterogeneity and is computed using a Fast-Marching Algorithm (FMA). In the following, we describe how the simulation medium is obtained and how the locations of the conduits are computed.

#### 3.4.1. Characterizing the simulation medium

To use the FMA, it is necessary to convert the geological information  $I_g$  (Eq. (1)) and the fracturation information  $I_f$  (Eq. (2)) in a velocity field  $K(\vec{x})$  [L/T] for each simulation of the fracture network and inception horizons.

We therefore convert the set of indicator functions obtained previously into a single velocity field. For that purpose, a velocity is defined for each of the different hydrogeological features: fractures and bedding planes are more conductive (high velocity) than matrix (low velocity). Aquitard formations have very low velocity. These velocities have the same units as hydraulic conductivities (m/s), but their values should be interpreted only as model parameters allowing to create contrasts between the different components of the propagation medium (matrix, fractures, inceptions horizons, etc.). In other words, these velocities control the shape of the network and must be adapted by the user to obtain a realistic geometry. A lower contrast leads to a network that will be mainly controlled by the position of the inlets and outlet, on the opposite a higher contrast leads to a network that will be mainly controlled by the shape of the initial heterogeneity.

Once these parameters are defined by the user, the velocity field for each simulation is obtained by computing the sum of the various components multiplied by their respective indicator functions:

$$K_0^S(\vec{x}) = \sum_{f=1}^{N_f} \left[ I_f^S(\vec{x}, f) \cdot K_f(f) \right] + \left( 1 - \sum_{f=1}^{N_f} I_f^S(\vec{x}, f) \right) * \left[ \sum_{g=1}^{n_g} (I_g(\vec{x}, g) \cdot K_G(g)) \right] \quad (10)$$

where  $K_G = \{k_1, k_2, \dots, k_{N_g}\}$  and  $K_f = \{k_{f1}, k_{f2}, \dots, k_{fN_f}\}$  are two arrays of length  $N_G$  and  $N_f$  (number of geological formations and number of fractures families) defining respectively the hydraulic conductivity (velocity) of every geological formation and every fracturation family. Eq. (10) assigns the velocity of the fractures at their simulated location within the medium and assigns otherwise the value associated to the corresponding geological formation.

#### 3.4.2. Conduit simulation, basic algorithm

The conduits are generated using a particle tracking approach within a 3D map of shortest time to the outlet. This map is computed using the Fast-Marching Algorithm (FMA) developed by Sethian (1996, 2001) and implemented by G. Peyré within the matlab Toolbox Fast Marching ([www.mathworks.com](http://www.mathworks.com)). The FMA is a front propagation algorithm. Here, we use the spring(s), i.e. the known outlet(s) of the aquifer, as the starting point for the propagation algorithm. The velocity of the front propagation at any point of the domain is given initially by the field  $K_0^S(\vec{x})$ . The result of the FMA is a 3D map of the time  $T_0^S(\vec{x})$  it has taken for the front to arrive in any point (pixels in 2D, voxels in 3D) of the domain from the outlets:

$$T_0^S(\vec{x}) = t(K_0^S, O^S) \quad (11)$$

where  $t$  represents the Fast Marching Algorithm. The next step consists in using the set of starting points locations  $\mathfrak{S}^S$  (Eq. (5)) generated previously. For each point in this set, we compute the path from the inlet toward the outlet by following the gradient of the

time map  $T_0^S(\vec{x})$ . In this way, the algorithm performs a particle tracking from points situated at the land surface ("starting points") and follow the shortest path from its starting point to the spring.

The tracks of the particles are stored via an indicator function  $I_c(\vec{x}, k)$  and describe the 3D karstic network through the domain:

$$I_c(\vec{x}, k) = \begin{cases} 1, & \text{if karst } k \text{ is present at location } \vec{x} \\ 0, & \text{otherwise} \end{cases} \quad (12)$$

By applying this algorithm iteratively, one can update the initial velocity field  $K_0^S(\vec{x})$  with the indicator function of karst conduits  $I_c(\vec{x}, k)$  and by defining  $K_{karst}$ , the velocity associated to the karst conduits. This allows generating a hierarchical karstic network that can include several phases of karstification. The resulting new velocity field is called  $K_i$  where  $i$  is the iteration number.

$$K_i^S(\vec{x}) = (I_c(\vec{x}, k) * K_{karst}) + (1 - I_c(\vec{x}, k)) * (K_{i-1}) \quad (13)$$

Consequently the 3D time map is updated for every iteration in this way:

$$T_i^S(\vec{x}) = t(K_i^S(\vec{x}), O^S) \quad (14)$$

As illustrated in Fig. 3b the first generation of conduits is influenced only by the initial heterogeneity of the media (Fig. 2a). Fig. 3c shows the network that is generated after three iterations. The hierarchical structure of karst conduits is respected because the pre-simulated network is a preferential path for the next walkers.

#### 3.4.3. Point or diffuse outlet

In real applications, it may be difficult to know on the field every single outlet of a karstic system. Sometimes outlets are located in diffuse areas and are therefore not represented by a single spring. To simulate this feature, it is possible to initialize the fast marching algorithm to start from a region instead of a single karst spring. i.e.  $O^S$  (Eq. (9)) is defined as a set of points defining a region and not as a single or a few points. This option can be interesting if one want to identify possible outlets of a region. Fig. 4 illustrate the results obtained using a single deterministic spring (located at the center of the inferior border of the image, Fig. 4a) and a diffuse spring zone (corresponding to the whole inferior border of the image Fig. 4b). Both simulations use the same fracture network and the same starting points for comparison. We notice that even when a diffuse outlet zone is used, the resulting networks still show a hierarchical structure. Because the locations of the springs are not imposed, they depend on fracture positions and interconnections only. These locations vary from one stochastic simulation to the next.

All the previous steps are summarized in Fig. 5 and constitutes the basic algorithm that we propose. It allows creating realistic conduit networks accounting for the regional geology and the internal heterogeneity. But this is not yet sufficient since it also needed to account for the unsaturated zone and for more complex situations such as multiple phases of karstifications. These questions are treated in the next sections.

#### 3.4.4. Accounting for the unsaturated zone

In 3D, the basic algorithm (Fig. 5) needs to be extended to account for the difference of structures in the unsaturated and saturated parts of the karstic systems. In the unsaturated zone (vadose zone), the main controlling factor is gravity, and the conduits are mainly collectors that drain the water concentrating from the epikarst (Huntoon, 1999). Therefore conduits are essentially vertical in the vadose zone, whereas in the saturated zone the conduits are essentially driven by the regional base level and the spring locations.

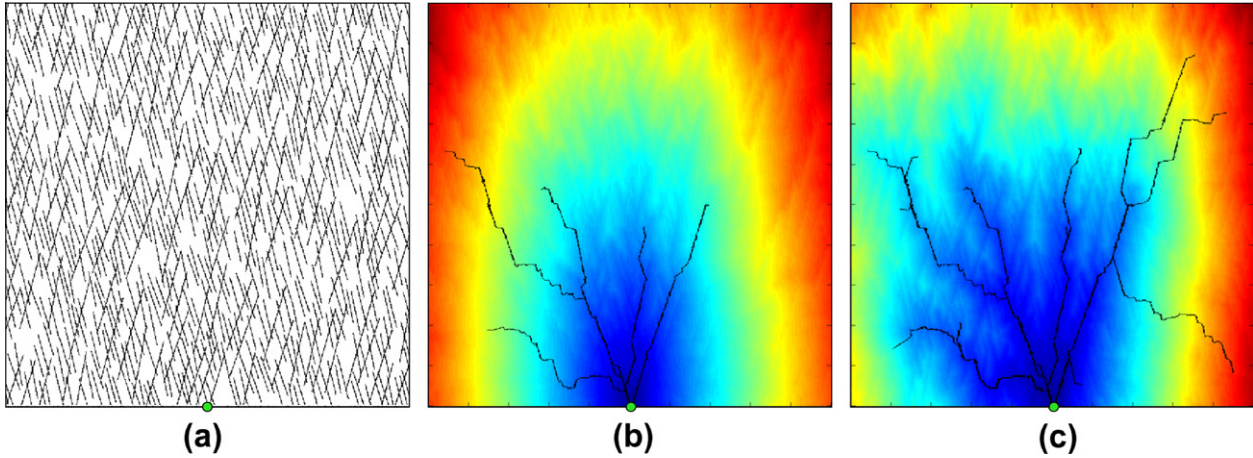


**Fig. 3.** (a) Initial fracture network, (b) first iteration of the algorithm, initial time map resulting of FMA from the spring location (green point) to every point of the domain. The black lines are the first conduits generated following the time map; color: blue (low values) to red (high values). (c) Third iteration of the algorithm. (For interpretation of the references to color in this figure legend, the reader is referred to the web version of this article.)

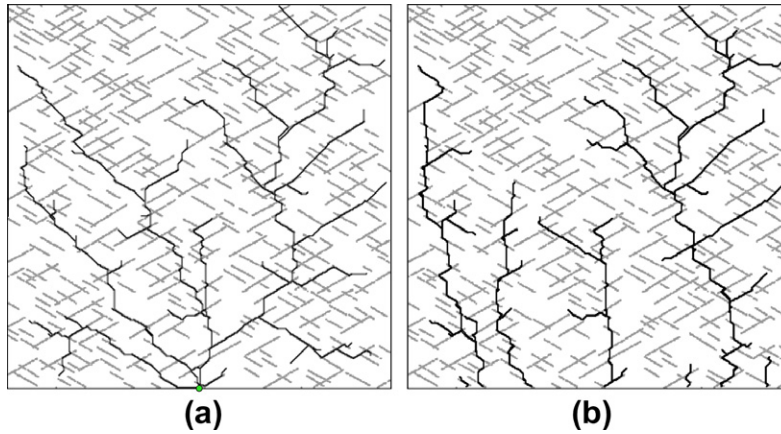


**Fig. 4.** Results of simulations on a 2D map. (a) Point deterministic spring (green point), (b) the whole bottom of the image is a zone of possible outlets, the real position of the outlet vary from one realization to the other. (For interpretation of the references to color in this figure legend, the reader is referred to the web version of this article.)

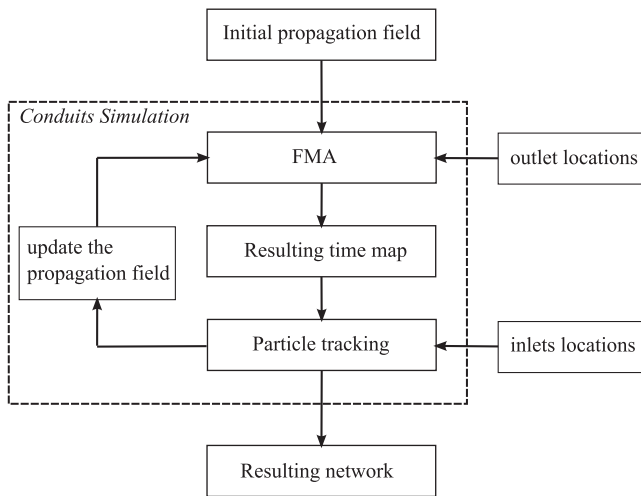


**Fig. 5.** Workflow of the basic algorithm for the generation of the karstic conduits using the Fast-Marching Algorithm (FMA).

To model those feature, the simulation process is divided in two steps: first the vadose conduits are generated and second the saturated ones (Fig. 6). Each step uses the basic algorithm described above (Fig. 5) but with different inlets and outlets.

For the first step, the initial front propagation points (diffuse outlet) correspond to a 2D surface: the base level that has been extended all over the 3D model. For a 2D cross section, it is a line or a curve (see dotted line in Fig. 6a):

$$O_{step1}^S = \{\bar{x}_{i1} = (x_{i1}, y_{i1}, z_{i1}) \text{ with } i1 \in (1, \dots, N_{XY})\} \quad (15)$$

where  $N_{XY}$  is the total number of points of the grid for one  $XY$  plane (i.e.  $N_{XY} = nx * ny$ , with  $nx$  and  $ny$  the grid dimensions in  $X$  and  $Y$  directions). Then, the FMA is used to compute the map of arrival times starting from the base plane  $O_{step1}^S$ :

$$T_{i1}^S(\vec{x}) = t(K_{i1}^S(\vec{x}), O_{step1}^S) \quad (16)$$

Particles are sent from the starting points  $\mathfrak{S}^S$  located on the topography. The result of the particle tracking is an indicator function of the presence of vadose conduits (Fig. 6a).

$$I_{vadose}(\vec{x}, vc) = \begin{cases} 1, & \text{if vadose conduits } vc \text{ is present at location } \vec{x} \\ 0, & \text{otherwise} \end{cases} \quad (17)$$

At the end of step 1, the set of coordinates of arrival locations of the particles on the base level  $O_{step1}^S$  is used as the set of starting points  $\mathfrak{S}_{step2}^S$  for the phreatic conduits in step 2.

Step 2 uses the FMA again, but now the starting locations for the front propagation are the actual outlets locations ( $O^S$ ) observed in

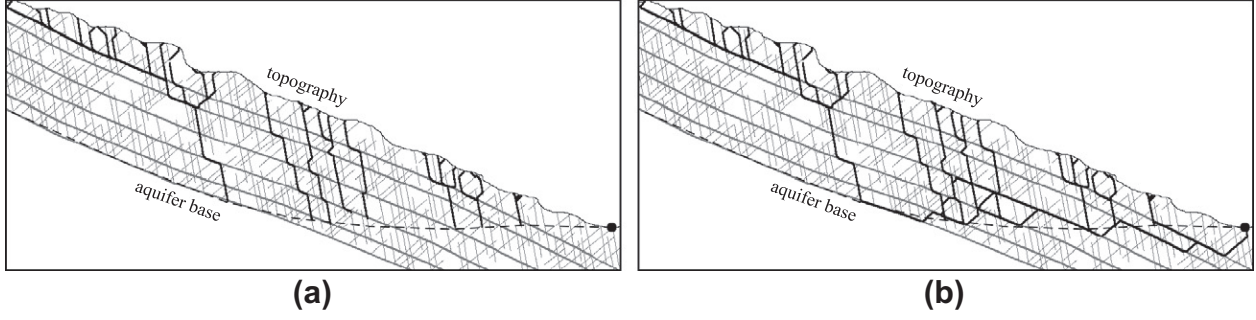


**Fig. 6.** Result of one 2D cross-section simulation: (a) the conduits (black lines) within the vadose zone are generated toward a base level first, (b) and then the saturated conduits are simulated toward the spring (b). The dotted line represent the phreatic surface. The filled circle represent the spring, the gray lines represent the fractures and the bedding planes.

the field. The resulting time map  $T_{i2}^S(\vec{x}) = t(K_{i2}^S(\vec{x}), O^S)$  is used to compute the paths from the starting points  $\mathfrak{S}_{step2}^S$  obtained in step 1. The result is the indicator function of the phreatic conduits:

$$I_{phreatic}(\vec{x}, pc) = \begin{cases} 1, & \text{if phreatic conduits } pc \text{ is present at location } \vec{x} \\ 0, & \text{otherwise} \end{cases} \quad (18)$$

We associate then the indicator function of vadose conduits  $I_{vadose}(\vec{x}, vc)$  (Eq. (17)) with the one of phreatic conduits  $I_{phreatic}(\vec{x}, pc)$  (Eq. (18)) to obtain the complete indicator function of the karst conduits  $I_c(\vec{x}, k)$  (Fig. 6b):

$$I_c(\vec{x}, k) = I_{vadose}(\vec{x}, vc) + I_{phreatic}(\vec{x}, pc) \quad (19)$$

#### 3.4.5. Complex connections between inlets and outlets

Karst aquifers are often characterized by springs alimanted by several sinkholes. But it can also occur that some of these sinkholes are connected to other springs as well. To simulate this type of relationship, the easiest way is to first simulate the network for one specific spring ( $O^S[1]$ ), and then for the second ( $O^S[2]$ ) and so on, keeping the result of every iteration as initial velocity field ( $K_i^S(\vec{x})$ ) for the next. In this way, it is possible to connect several springs  $O^S [1, \dots, n]$  to several sinkholes in a very simple way (Fig. 7).

#### 3.4.6. Multiple phases of karstification

If different phases of karstification have to be accounted for due to the existence of different paleo hydrological conditions, the generation of karst networks can be repeated several times using the

pre-simulated network as an initial velocity field ( $K_i^S(\vec{x})$ ) and changing the FMA initial front propagation points  $O^S$  for every change in the paleo conditions. Fig. 8 illustrate this method on a simple 2D system assuming the presence of two phases of karstification with two successive springs corresponding to two distinct base levels.

#### 3.4.7. Hierarchical ordering of the conduit

The algorithm described above allows to compute a conduit order, which depends on the total catchment area drained by the conduit. The whole network is divided in a set of topological segments. Each segment is defined as a portion of the network bounded by two branching or diverging connections without any internal connection. Every segment  $j$  inherit its order  $\omega_j$  (expressed in %) from the upstream segments (Fig. 9). It can be computed as the sum of the indicator functions of presence for each conduit  $I_{ci}$  (i.e. its full path from the inlet toward the spring) of the upstream conduits multiplied by the importance factor  $w_i^3$  (see Eq. (6)) of its corresponding inlet.

$$\omega_j = \sum_{i=1}^{N_3} I_{ci} * w_i^3 \quad \forall j \in (1, \dots, N_s) \quad (20)$$

#### 3.5. Stochasticity of the generated networks

Despite of the influence of the geological model which controls the regional shape of the networks, the generation of conduits networks has three main levels of stochasticity.

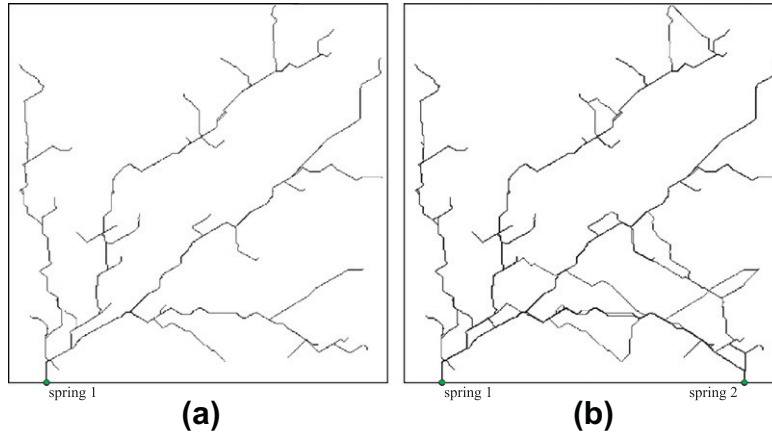


**Fig. 7.** 2D map. To simulate multiple connections we first develop a whole network for the first spring (a) and then the one for the second spring (b), keeping the first one to create a complex multi-connected network.

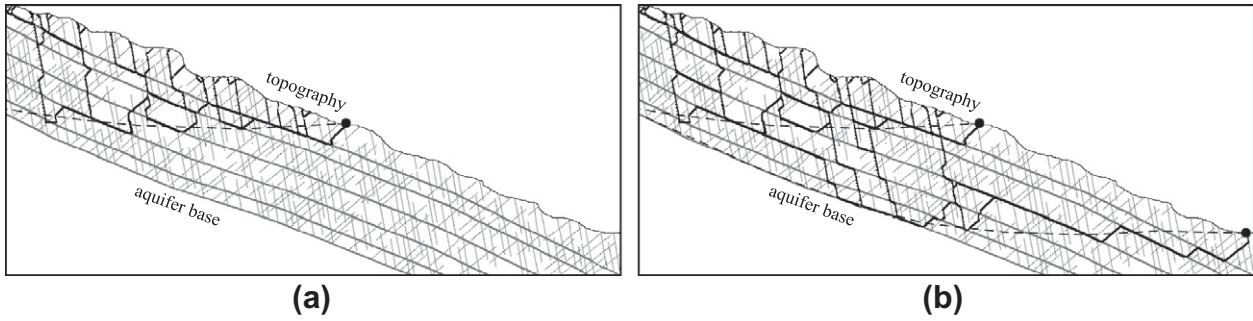


**Fig. 8.** 2D cross-section of multi-phase karstification. Two successive speleogenetic phases are illustrated. The dotted line represent both phreatic surfaces, the old (a) and the actual (b). The filled circles represent the springs, the gray lines represent the fractures and the bedding planes, black lines represent the conduits.

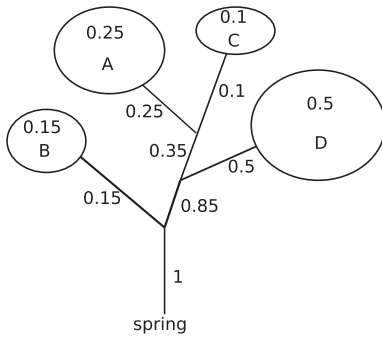


**Fig. 9.** Schematic illustration of the conduit ordering. Every conduit inherit the rank (in % of total catchment drained surface) of the upstream conduit or inlet (A–D).

The first level depends on the stochastic model of inlet locations  $\mathfrak{S}_p^s$ . Since not all the inlets of the model are precisely known, they are modeled by a point process which can be parametrized by a map of a probability of occurrence of an inlet  $P_i(x,y)$  (Section 3.3).

The second level depends on the stochastic model of fractures. Fig. 10 illustrate equiprobable realizations obtained using the same inlets and outlet, but using three equiprobable realizations for fractures (gray lines). The paths of the resulting conduits (black lines) and their interconnections vary significantly. Furthermore, one can test several models of fractures to investigate the uncertainty related to the fracturation model itself.

Finally, the third level depends on the stochastic model of the outlets of the system  $O_p^s$ . Despite they are often known, one can generate models also in the case where there are no information

about the outlets of the system, like in the Damour example (Section 4.1).

#### 4. 3D demonstrative examples

This section provides two illustrations of the applications of the proposed methodology. The aim of the paper is to develop a conceptual framework and a numerical method but not to provide a detailed and accurate model of the regions that are used for the test. This is why we show the following examples only to demonstrate the applicability of the method and we use them to identify the work that remains to be done to represent as accurately as possible a real system.

##### 4.1. Case 1, coastal aquifer

This first example illustrates the application of the methodology to a synthetic case, representing a typical kind of karstic coastal aquifer on the Mediterranean basin. The basic geology is inspired by the Damour region in Lebanon. Even if that specific region is known to be only moderately karstified, its geological structure is a good analog of many other aquifers along the Mediterranean that are well karstified and often present submarine karstic springs (Fleury et al., 2007).

We show how to use the proposed methodology, with multiple phases of karstification due to the variation of the base level caused by glaciations. The lowest sea level known below the present occurred during the Würm glacial maximum (Ford and Williams, 2007). It was between  $-120$  to  $-140$  m. Thus, we modeled two dis-

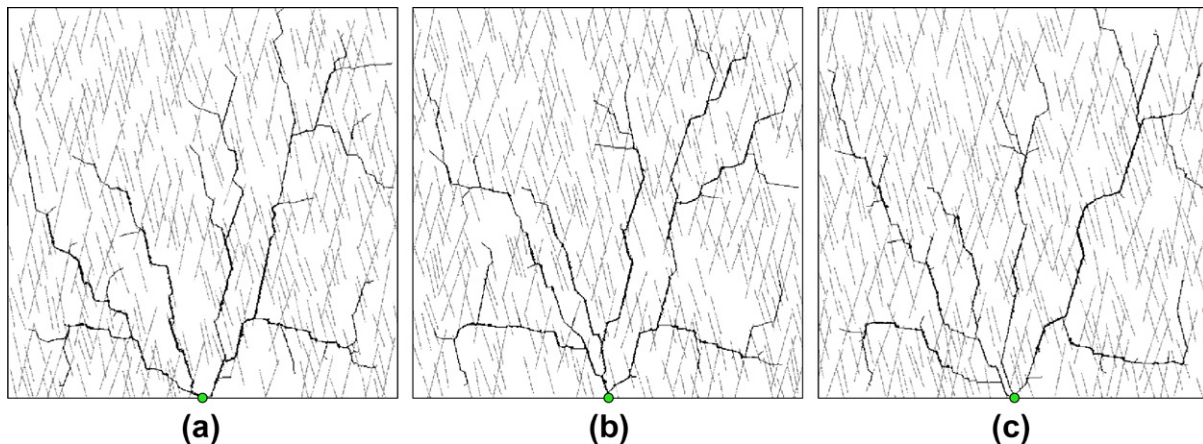


**Fig. 10.** Three different equiprobable realizations (2D map), the outlet (green point) and the inlets (starting points of the conduits, black lines) are the same for all the realizations. The different equiprobable fracture network (gray lines) influence the connectivity of the resulting network. (For interpretation of the references to color in this figure legend, the reader is referred to the web version of this article.)

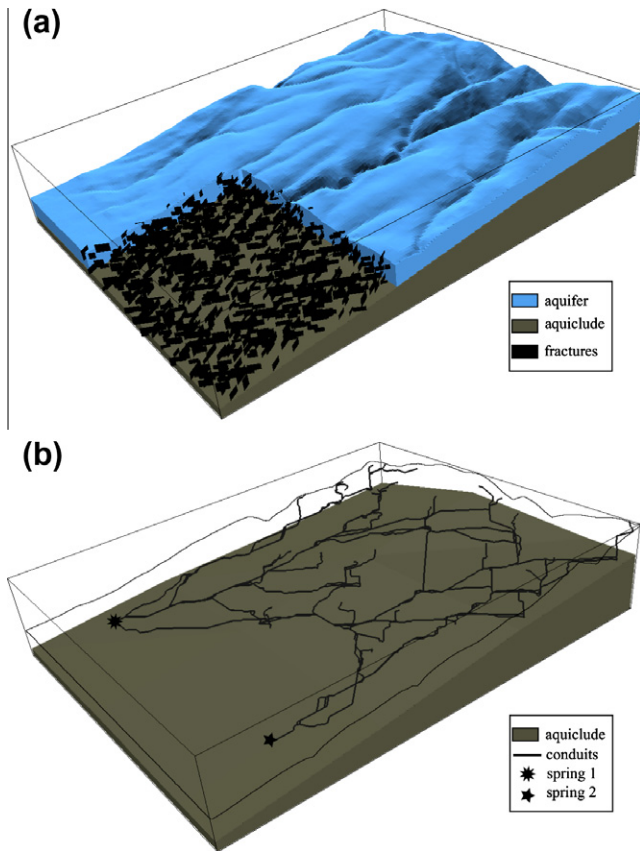


**Fig. 11.** Coastal aquifer example. (a) Geological model with fractures, showing also both basal levels (-140 m and 0 m) (b), karst system for paleo base level (-150 m), karst system under actual conditions (base level = 0 m).

tinct phases of karstification, one with the sea (base) level at -140 m and one at 0 m. The network resulting from the first simulation is kept for the second stage, so that conduits will be reactivated during the second stage.

The geology of the site is relatively regular. In the western part of the model (i.e. seaside), the structure is mainly homoclinal, dipping Westward at an angle between 30° and 50° following the topography. Towards the mountains, the structure rises to the surface at an angle of 90° (Fig. 11a).

We had no field information about fracturation, so (because it is a synthetic case) we assumed two families of fractures due to the compression that resulted in the folding. Considering a syncline axis (Eastern part of the model, in the mountains) oriented N-S, we can assume two families of conjugated faults oriented at 60° degrees one from each other: one NW-SE (strike 345°N) and one SW-NE (strike 15°N). The fractures are assumed to be vertical, their mean length is 250 m and their mean vertical extension is 150 m (Fig. 11a).

For every karstification stage, the spring location has been chosen randomly on the coastline at a depth of 15 m below the respective base level, like one of the springs of the analog aquifer of Gekka, Lebanon (El-Hajj et al., 2006).

Because it is a synthetic case, we simply assume that the probability distribution for the starting points of the conduits  $\mathfrak{F}_p^s$  (Eq. (4)) is uniform at the land surface where karstic formations are outcropping. The number of starting points for the conduits is  $h = \{5, 10, 20\}$ , i.e. 5 for the first iteration, 10 for the second and 20 for the last one. We assume for this example that the paleo inlets are the same as the actual ones. Fig. 11b shows one resulting network.

#### 4.2. Case 2, aquifer in folded tectonics

The second example corresponds to a karstic system developed in a more complex tectonic setting. The studied site is the catchment of the Noiraigue spring in the Swiss Jura mountains, close to city of Neuchâtel. This karstic system cannot be explored by speleologist. The site has however been studied for decades at the university of Neuchâtel by hydrogeologists (Gillmann, 2007; Gogniat, 1995; Morel, 1976) and geologists (Sommaruga, 1996; Valley et al., 2004). It is characterized by a highly folded geology with complex overthrusting. The catchment of the Noiraigue spring is a dry syncline valley, called “Vallée des Ponts-de-Martel”; all the precipitation falling on the valley infiltrates into the karst system and the only known outlet of the system is the Noiraigue spring, so we defined it deterministically as the only output point of the domain. The catchment area is approximately 70 square km and is delimited by two overthrusting anticlines.

To build the 3D model of the regional geology of the catchment (Fig. 12a), we used more than 50 interpreted cross-sections (Sommaruga, 1996; Valley et al., 2004), part of three seismic profiles, six boreholes and four different geological maps (interpretation) of the region (Borghi, 2008). These data were imported in the software Geomodeller3D (Calcagno et al., 2008) and used to interpolate the 3D geometry of the main structures including the lithological formations, folds, thrusts and faults.

There are several families of conjugated faults that can be observed in the field due to folding, but we retained only the major ones, i.e. WNW-ESE (strike = 300°N) and N-S (strike = 0°N) according to Sommaruga (1996) for the model. Similarly to example 1 (Section 4.1) we used a Boolean technique to generate the fractures (Fig. 12b).

The probability of occurrence of the starting points of the conduits is uniformly distributed at the land surface within the catchment but only where karstic formations are outcropping. In addition, eight major known inlets (sinkholes and dolines) are defined deterministically.

We then simulated the network by first simulating the vadose conduits and second the phreatic ones (see Section 3.4.4). For the vadose conduits, we assumed the base level to be the plane at the same altitude of the spring and crossing the whole catchment.

As expected, the resulting networks follow the geometry of the main geological structures (Fig. 12c). They are well constrained by the known locations of inlets and the outlet. The main conduits cross the aquifer underneath the tertiary aquitard as supposed by the existing hydrogeological analyses of the region (Gogniat, 1995; Morel, 1976). We therefore obtain a reasonable 3D model of the conduits in a very complex geological setting.

To increase the reliability of this model, we would need to better constrain the fracturation model and use a more advanced tool for the generation of the fracturation that would account for the known folds and thrusts. We would also need to improve the stochastic model of potential inlet locations since geomorphological information is available in surface. This work will certainly constitute a direction for future research.

## 5. Discussion

In this paper, we present a new stochastic methodology to model karst reservoirs. This method is significantly different from the ones found in literature. Its main strength is that it allows integrating a broad range of data and conceptual knowledge into a single stochastic model. The regional geology can be accounted for even when it is very complex. The method allows to condition the karst conduit model with actual observations. If inlets or outlets are known on the field it is sufficient to set them as starting or ending

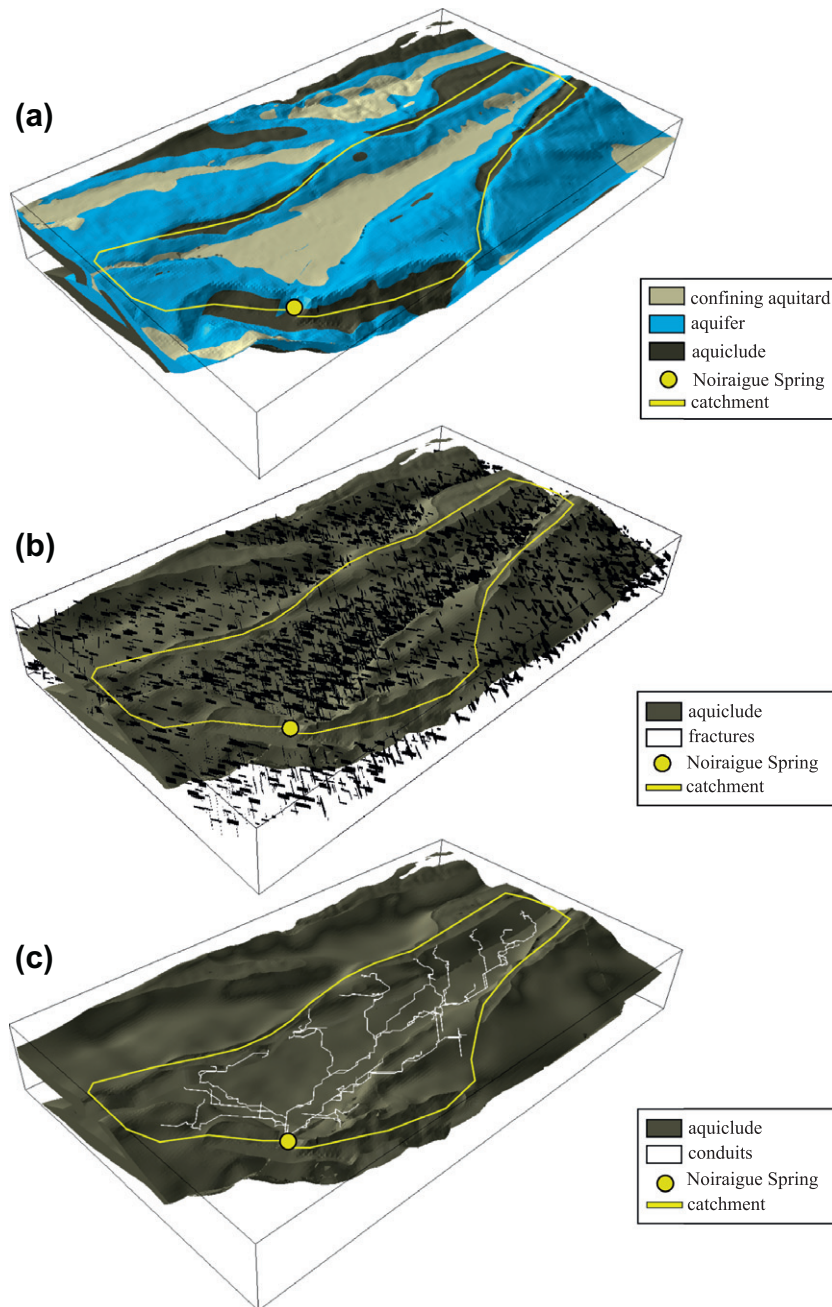


**Fig. 12.** Folded aquifer. (a) Geological model, (b) fracture model, (c) resulting network, (d) resulting network with aquitard. The conduits follow the regional geology and the local fracturation.

points in a deterministic way. Borehole data confirming the presence of conduits can be used as well. The method can handle the existence of different phases of karstification and the distinction between the vadose and phreatic zones. When some information is only available in a probabilistic manner, the method allows to account for it and is able to generate an ensemble of realizations representing the uncertainty on the true position or structure of the network.

For the moment, the geological model is defined in a deterministic way. The resulting model reflects the vision that the modeler has of a specific site. It is therefore a good practice to build several geological models if different assumptions can be made related to the geological structure. By doing different models one can use the proposed approach to test the plausibility of different assumptions, and evaluate their influence on the subsequent processes. In addition,

it is very important to have a good model for the fracturation and other heterogeneities like the bedding planes. This requires accurate field measurements and observations as well as a numerical tool able to include those observations into the model. Some additional work is required in that direction. But it does not change the principle of the proposed model.

The heart of the methodology relies on the use of the Fast Marching Algorithm. Alternatively, one could use groundwater flow simulations and compute streamlines to obtain similar results. Both techniques have pros and cons. As a first guess, using a flow simulation may seem better. Flow is the physical process controlling the speleogenesis and could therefore seem easier to justify. But in fact, it is more difficult to use because one has to define the flow parameters of the different geological materials (matrix, fractures and conduits) and the boundary conditions. The FMA

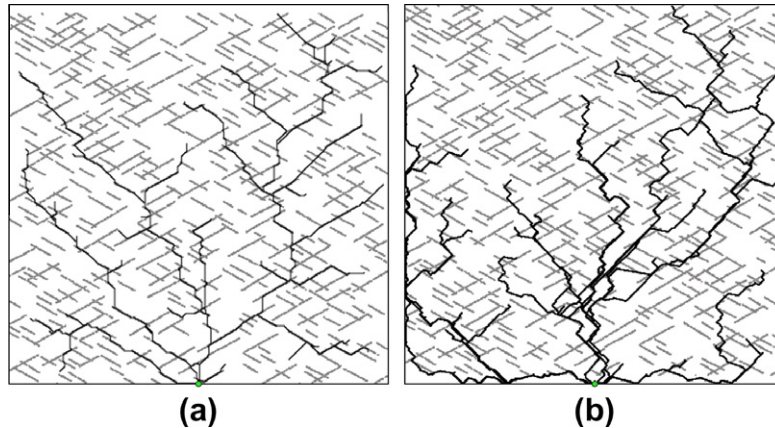


**Fig. 13.** Conduits generated using: (a) the Fast Marching Algorithm and (b) a steady state flow simulation. For case b an uniform source term has been applied on all the model surface, and a constant head boundary condition has been applied at spring location. We notice that using a flow simulation we obtain a network which is slightly more “rounded” and more influenced by the border of the model (no flow borders).

is much simpler to apply. To evaluate the impact of the two options, we made several tests in 2D. One of the comparison between FMA and flow simulation is shown in Fig. 13. The flow simulation was computed with a constant and uniform source term on the whole domain, a constant head boundary condition at the spring location and a no-flow boundary on the sides. A difference of five orders of magnitude is prescribed between the hydraulic conductivity of the matrix and of the fractures and one additional order of magnitude between the fractures and the conduits. The flow paths are influenced by this strong heterogeneity and so do the conduits. In this case, the comparison of Fig. 13a and b shows that the shape of the conduits obtained from the flow simulation is less influenced by the fracture position than those obtained from the FMA (Fig. 13a). Furthermore the flow simulation is also strongly influenced by the no-flow boundaries on the sides of the model. In this situation, using the flow simulation generates more geometrical artifacts than the FMA. The flow simulations are also more CPU demanding, one simulation for this  $500 \times 500$  2D simulation takes less than 10 s using the FMA (PC: dual-core 2.4 GHz, 2 Gb Ram) and about 3 min using a steady state flow simulation (without writing the output files). In 3D, accounting for the vadose zone would be even more complicated since it would require solving the unsaturated flow equations on very large grids. Due to the nonlinearity of those equations, this can become extremely CPU intensive and not applicable in a stochastic context as shown by Brunner et al. (2010). For all those reasons, we prefer to use the Fast Marching Algorithm which simply computes the shortest path. This is certainly a reasonable physical approximation for our purpose.

As the FMA is only an approximation, it has to be applied carefully. For example, artifacts can occur if the karst formation is folded. The worst artifacts that we obtained were conduits going upward. It may occur if a starting point has been defined in a hole, and so following the time map computed by the FMA, the conduit may go upward. To avoid this kind of artifacts, a great attention has to be accorded to the definition of the starting points probability map.

Another problem happens in 3D when conduits follow the “gravity” in the vadose zone (step 1 explained in Section 3.4.4). If the base level for the FMA  $Sl_1$  (Eq. (11)) is badly defined, or if it is located outside of the aquifer limit, the conduits can be “attracted” toward aberrant zones. The modeler has to accurately investigate the resulting networks, and a good interpretation is essential. Actually, this feature can be used to test the extension of a catchment: points located outside the catchment will generate conduits that will leave the catchment.

Moreover, in real karst systems, the development of the unsaturated and saturated zone are synchronous and follow several successive phases of maturation (Filipponi, 2009). In our approach, we approximate this behavior by simulating only mature karst systems, that have already reached the equilibrium. With this assumption, simulating first all the vadose conduits and in a second step the phreatic ones leads to a geometrical reconstruction of the mature karst that is coherent with the actual conceptual model (Ford and Williams, 2007).

As we already mentioned in the introduction, the proposed approach aims at generating karst conduits networks and not cave geometry like Henrion et al. (2008). In real karst aquifers, huge caves can be present, but we do not consider them yet in our approach because we work on regular grids. At a regional scale, the resolution of the grid is often coarser than the dimensions of the caves (cell resolution  $\geq 50$  m). Therefore, the caves can be represented only by “conduit” elements. Instead of trying to model the detailed geometry of the caves, we think that it is more reasonable to pursue our work in the future by defining a model of the radius (or rugosity) of the conduits that will be computed all along the conduit networks. A reasonable model for the radius will be to relate statistically the conduit order defined above (Eq. 20) with its radius using a power law. For similar reasons, we do not simulate the epikarst and its internal detailed heterogeneity using discrete features. Instead, in a regional flow model we think that it is more reasonable to represent the epikarst by a highly conductive layer (that can be heterogeneous) at the topographical surface of the model.

Another important point that needs to be discussed is that the number of conduits and the different phases of karstification are for the moment controlled by the user. He has to define those parameters. As speleogenetic process based simulations show (Dreybrodt et al., 2005) the dissolution in natural system is very active when the head gradient is high. Because of the dissolution, the hydraulic resistance of the medium tends to decrease and the gradient decreases (the rate of precipitation or inflow is supposed to remain constant) until the system reaches a breakthrough point. This determines the moment after which the karst network is in equilibrium with the inflow, i.e. all the infiltrated water is drained easily by the system. After the breakthrough, the dissolution is more active in the epikarst and the geometry of the main network does not change that much anymore. Using the pseudo-genetic approach, we do not account for this factor because we do not model the dissolution processes. Instead, the user has to control that the parameters that were used to build a reasonable network. In this

process, the importance factor (Sections 3.3.1 and 3.4.7) can be used as a criteria controlling the density of the inlets: using a DEM analysis tool, as the drainage surface of every inlet is already estimated; the algorithm could proceed by adding inlets on the surface until the sum of the drained surface is equal to a user defined threshold. This idea needs to be tested in detail and is therefore not yet implemented in the code.

## 6. Conclusions and outlooks

We propose an integrated method to model epigenetic karst reservoirs. It allows honoring conceptual knowledge existing about karst and speleogenesis processes as well as most of the available field data. As far as we know this is the first stochastic method allowing to account for several phases of karstification and to distinguish the saturated and unsaturated zones. The method is very flexible and numerically efficient thanks to the use of approximated physics concepts and it belongs therefore to the pseudo-genetic class of stochastic models. The use of the Fast Marching Algorithm to perform the search of minimum effort paths allows to simulate realistic conduits in a very CPU efficient manner.

The proposed model is a tool allowing to test different assumptions concerning either the regional geology, the fracturation, the inception horizon or the hydrogeological control of the system. It generates conduits that can be used to generate finite element or finite differences mesh which can be used to model flow and transport in the karst system. The model is stochastic and allows to investigate the uncertainty related to a current state of knowledge and data availability.

As any model, its underlying parameters have to be inferred from field observations. Some parameters can be directly derived from the measurements (location of the springs for example), some other parameters are not necessarily directly measurable (number of major stages of karstification for example). Depending on the parameters used in the model one can obtain a very wide range of structures from curvilinear branching network to anastomotic mazes.

For the moment, a trial and error procedure is used to select the parameters. By testing the impact of those parameters and checking visually if the resulting networks are reasonable, one can obtain the type of network that is expected. In the future, the methodology will have to include a calibration procedure based on a number of statistical measures describing the topology and geometry of the network. Those measures will be used to compare the simulated networks with observed ones in order to test the validity of the selected model parameters.

## Acknowledgements

This research was funded by Schlumberger Water Services. We thank J.-P. Delhomme who initiated the project and always gave passionate feed-back, G. Mathieu who continuously supported the project. A. Comunian, P. Brunner and three anonymous reviewers helped us making the manuscript more understandable.

## References

Attea, O., Perret, D., Adatte, T., Kozel, R., Rossi, P., 1998. Characterization of natural collodis from a river and spring in a karstic basin. *Environ. Geol.* 34 (4), 257–269.

Bakalowicz, M., 2005. Karst groundwater: a challenge for new resources. *Hydrogeol. J.*, 13.

Biondic, B., Bakalowicz, M., 1995. COST action 65 – hydrogeological aspects of groundwater protection in karstic areas. Final report.

Borghesi, A., 2008. Modélisation 3D d'un aquifère karstique, la Vallée des Ponts-de-Martel et la source de la Noiraigue, University of Neuchâtel, Neuchâtel.

Bour, O., Davy, P., Darcel, C., Odling, N.E., 2002. A statistical scaling model for fracture network geometry, with validation on a multiscale mapping of a joint network (Hornelen Basin, Norway). *J. Geophys. Res.* 107 (B6), 10.1029/2001JB000176.

Brunner, P., Simmons, C.T., Cook, P.G., Therrien, R., 2010. Modeling surface water-groundwater interaction with MODFLOW: Some considerations. *Ground Water* 48, 174–180.

Calcagno, P., Chièss, J.P., Courrioux, G., Guillen, A., 2008. Geological modelling from field data and geological knowledge: Part I. Modelling method coupling 3D potential-field interpolation and geological rules. *Phys. Earth Planet. Interiors* 171 (1–4), 147–157.

Camac, B.A., Hunt, S.R., 2009. Predicting the regional distribution of fracture networks using the distinct element numerical method. *AAPG Bull.* 93 (11).

Castaing, C. et al., 2002. Taking into account the complexity of natural fracture systems in reservoir single-phase flow modelling. *J. Hydrol.* 266, 15.

Caumon, G., Collon-Drouaillet, P., Le Carlier de Veslud, C., Viseur, S., Sausse, J., 2009. Surface-based 3D modeling of geological structures. *Math. Geosci.* 41 (8), 927–945.

Cornaton, F., Perrochet, P., 2002. Analytical 1D dual-porosity equivalent solutions to 3D discrete single-continuum models. Application to karstic spring hydrograph modelling. *J. Hydrol.* 262 (1–4), 165–176.

Dreybrodt, W., Gabrovsek, F., Douchko, R., 2005. Processes of speleogenesis: a modelling approach. *Carsologica. Karst research institute ZRC Postojna – Ljubljana.*

Eisenlohr, L., Bouzelboudjen, M., Kiraly, L., Rossier, Y., 1997. Numerical versus statistical modelling of natural response of a karst hydrogeological system. *J. Hydrol.* 202 (1–4), 244–262.

El-Hajj, A., Bakalowicz, M., Najem, W., 2006. Hydrogéologie des calcaires crétacés du Nord Liban. In: *The 3rd International Conference on the "Water Resources in the Mediterranean Basin". WATMED 3, Tripoli, Lebanon*, p. 210.

Filipponi, M., 2009. Spatial analysis of karst conduit networks and determination of parameters controlling the speleogenesis along preferential lithostratigraphic horizons, EPFL – Ecole Polytechnique Fédérale de Lausanne, Lausanne – Switzerland, 130 pp.

Filipponi, M., Jeannin, P.-Y., 2010. Karst-ALEA: a scientific based karst risk assessment for underground engineering. In: *Andreo, B., Carrasco, F., Duran, J.J., LaMoreaux, J.W. (Eds.), Advances in Research in Karst Media. Environmental Earth Sciences. Springer, Berlin, Heidelberg*, pp. 435–440.

Filipponi, M., Jeannin, P.-Y., Tacher, L., 2009. Evidence of inception horizons in karst conduit networks. *Geomorphology* 106 (1–2), 86–99.

Fleury, P., Bakalowicz, M., de Marsily, G., 2007. Submarine springs and coastal karst aquifers: a review. *J. Hydrol.* 339 (1–2), 79–92.

Ford, D., Williams, P., 2007. *Karst Hydrogeology and Geomorphology*. John Wiley and Sons, Ltd., Chichester, England, p. 562.

Ghosh, K., Mitra, S., 2009. Two-dimensional simulation of controls of fracture parameters on fracture connectivity. *AAPG Bull.* 93 (11).

Gillespie, P., Howard, C.B., Walsh, J.J., Watterson, J., 1993. Measurement and characterisation of spatial distributions of fractures. *Tectonophysics* 226, 28.

Gillmann, A., 2007. Etude du comportement des substances particulières et solubles dans un système karstique de la source de la Noiraigue, Neuchâtel.

Gogniat, S., 1995. Etude des infiltrations rapides de l'aquifère de la Noiraigue (Neuchâtel, Suisse), approche par jeaugeages et multitraçages, Neuchâtel.

Gringarten, E., 1998. Fracnet: stochastic simulation of fractures in layered systems. *Comput Geosci* 24 (8), 8.

Henrion et al., 2010. *An Object-Distance Simulation Method for Complex Natural Structures*, vol. 42. Springer, Heidelberg, Allemagne.

Henrion, V., Pellerin, J., Caumon, G., 2008. A stochastic methodology for 3D cave system modeling. In: *Ortiz, J.M., Emery, X. (Eds.), Geostats 2008. Proceedings of the Eighth International Geostatistics Congress. Gecamin, Santiago, Chile*, pp. 525–534.

Hill, M.E., Stewart, M.T., Martin, A., 2010. Evaluation of the MODFLOW-2005 conduit flow process. *Ground Water* 48 (4), 559.

Huntoon, P., 1999. Karstic permeability: organized flow pathways created by circulation. In: *Palmer, A.N., Palmer, M.V., Sasowsky, I.D. (Eds.), Karst Water Resources, Charlottesville, Virginia*.

Jaquet, O., Siegel, P., Klubertanz, G., Benabderrhamane, H., 2004. Stochastic discrete model of karstic networks. *Adv. Water Res.* 27, 751–760.

Jeannin, P.-Y., 1996. Structure et comportement hydraulique des aquifères karstiques. University of Neuchâtel, Neuchâtel, 244 pp.

Jourde, H., Cornaton, F., Pistre, S., Bidaux, P., 2002. Flow behavior in a dual fracture network. *J. Hydrol.* 266 (1–2), 99–119.

Käss, W., 1998. *Tracing Technique in Geohydrology*. Balkema, Rotterdam, 572 pp.

Kaufmann, G., 2009. Modelling Karst Geomorphology on Different Time Scales. Elsevier, Amsterdam, Pays-Bas, 16 pp.

Kaufmann, G., Braun, J., 2000. Karst aquifer evolution in fractured, porous rocks. *Water Resour. Res.* 36 (6), 1381–1391.

Kiraly, L., 1979. Remarques sur la simulation des failles et du réseau karstique par éléments finis dans les modèles d'écoulement. *Bull. Centre Hydrogéol.* 3, 155–167.

Kiraly, L., 1988. Large scale 3-D groundwater flow modelling in highly heterogeneous geologic medium. In: *Custodio, E. (Ed.), Groundwater Flow and Quality Modelling*. D. Reidel Publishing Co., Boston, pp. 61–775.

Kiraly, L., Mathey, B., Tripet, J.-P., 1971. Fissuration et orientation des cavités souterraines: région de la Grotte de Milandre (Jura tabulaire). *Bull. Soc. Neuchâteloise Sci. Nat.* 94, 15.

Klimchouk, A., 2007. Hypogene Speleogenesis: Hydrogeological and Morphogenetic Perspectives, Carslbad.

- Lajaunie, C., Courrioux, G., Manuel, L., 1997. Foliations field and 3D cartography in geology: principles of a method based on potential interpolation. *Math. Geol.* 29 (4), 571–584.
- Lamelas, M.T., Marinoni, O., Hoppe, A., de la Riva, J., 2007. Doline probability map using logistic regression and GIS technology in the central Ebro Basin (Spain). *Environ. Geol.* 54, 15.
- Leibundgut, C., Maloszewski, P., Külls, C., 2009. Tracers in Hydrology, p. 432.
- Mallet, J.-L., 2002. *Geomodeling. Applied Geostatistics Series.* Oxford University Press, 624.
- Morel, G., 1976. Etude hydrogéologique du bassin de la source de la Noiraigue, internal report. CHYN, Neuchâtel.
- Palmer, A.N., 1991. Origin and morphology of limestone caves. *Geol. Soc. Am. Bull.*, 103.
- Ronayne, M.J., Gorelick, S.M., 2006. Effective permeability of porous media containing branching channel networks. *Phys. Rev. E: Stat. Nonlin. Soft Matter Phys.* 73 (2 Pt 2), 026305.
- Sauter, M., Kovacs, A., Geyer, T., Teutsch, G., 2006. Modelling karst groundwater hydraulics – an overview. *Grundwasser* 11 (3), 143–156.
- Schwanghart, W., Kuhn, N.J., 2010. TopoToolbox: a set of matlab functions for topographic analysis. *Environ. Model. Software*, 25.
- Sethian, J.A., 1996. A fast marching level set method for monotonically advancing fronts. *Proc. Natl. Acad. Sci. USA* 93 (February).
- Sethian, J.A., 1999. *Level Set Methods and Fast Marching Methods Evolving Interfaces in Computational Geometry, Fluid Mechanics, Computer Vision, and Materials Science.* Cambridge University Press.
- Sethian, J.A., 2001. Evolution, implementation, and application of level set and fast marching methods for advancing fronts. *J. Comput. Phys.* 169 (2), 503–555.
- Sharp, I., Gillespie, P., Lonoy, A., Horn, S., Morsalnezhad, D., 2006. Outcrop characterization of fractured cretaceous carbonate reservoirs, Zagros Mountains, Iran, first international oil conference and exhibition. SPE international, Cancun (Mexico).
- Sommaruga, A., 1996. Geology of the central Jura and the molasse basin: new insight into an evaporite-based foreland fold and thrust belt, Neuchâtel.
- Valley, B., Burkhard, M., Schnegg, P.-A., 2004. Dépliage 3-D des anticlinaux bordant le synclinal fermé de la vallée des Ponts, Jura central, Suisse. *Ecolae Geol. Helv.* 97, 279–291.
- Worthington, S.R.H., 1999. A comprehensive strategy for understanding flow in carbonate aquifers. In: Palmer, A.N., Palmer, M.V., Sasowsky, I.D. (Eds.), *Karst Modelling.* Karst Water Institute, Charles Town, WV.
- Worthington, S.R.H., Ford, D.C., Beddows, P.A., 2000. Porosity and permeability enhancement in unconfined carbonate aquifers as a result of solution. In: Klimchouk, A., Ford, D., Palmer, A., Dreybrodt, W. (Eds.), *Speleogenesis: Evolution of Karst Aquifers.* National Speleological Society, p. 527.